Synthesis and Excited State Spectroscopy of Tris(distyrylbenzenyl)amine-cored Electroluminescent Dendrimers

Lars-Olof Pålsson,[†] Richard Beavington,[‡] Michael J. Frampton,[‡] John M. Lupton,[§] Steven W. Magennis,[§] Jonathan P. J. Markham,[§] Jonathan N. G. Pillow,[‡] Paul L. Burn,*[,‡] and Ifor D. W. Samuel*[,§]

Department of Physics, University of Durham, South Road, Durham, DH1 3LE, U.K.; The Dyson Perrins Laboratory, Oxford University, South Parks Road, OX1 3QY, Oxford, U.K.; and Organic Semiconductor Centre, School of Physics and Astronomy, University of St. Andrews, North Haugh, St. Andrews, Fife, KY16 9SS, U.K.

Received November 15, 2001; Revised Manuscript Received July 19, 2002

ABSTRACT: An efficient strategy has been developed for the preparation of four generations of electroluminescent dendrimers that contain tris(distyrylbenzenyl)amine cores, stilbene dendrons, and *tert*-butyl surface groups. The synthesis involved coupling of benzylphosphonate focused dendrons with tris(4′-formylstilbenyl)amine to give the dendrimers in yields ranging from 63 to 86%. The dendrimers were found to be monodisperse by gel-permeation chromatography. The zeroeth generation dendrimer underwent two chemically reversible oxidations while for the higher generations only one chemically reversible oxidation was observed. On reduction, the dendrimers were found to aggregate with the level of aggregation dependent on the switching potential. The four dendrimer generations were investigated by means of optical spectroscopy. Time-resolved luminescence of the dendrimers in solution showed that the excited state of each of the generations had a monoexponential decay with a lifetime of 1.8 ns. The photoluminescence quantum yield (PLQY) of the dendrimers in solution was independent of generation and was found to be in the region of 0.62. This suggests that the origin of the luminescence is the same for all dendrimer generations. In thin films, time-resolved luminescence of the zeroeth dendrimer generation revealed a long-lived luminescence component in the red part of the spectrum with a lifetime of 7.5 ns. This emission component could not be found in the first, second, and third generation dendrimers, where the long-lived luminescence had a lifetime of 1.5−3 ns at all detection wavelengths. Furthermore, the PLQY of the dendrimer films was found to be dependent on generation and significantly lower than the solution PLQYs. The dendrimer film PLQY increased with generation from 5% for the zereoth generation to 12% for the third generation. The differences observed in the time-resolved luminescence and PLQY of the dendrimers in the solid state arise from the fact that intermolecular interactions between the emissive cores of the dendrimers are considerably stronger in the zeroeth generation than in higher generations. The intermolecular interactions result in an aggregate, which we ascribe to an excited-state species, such as an excimer.

Introduction

Electroluminescent dendrimers are an exciting new class of materials for organic light-emitting diodes (OLEDs).[1−4] Dendrimers have distinct advantages over the two traditional classes of materials used as the light-emitting layer in OLEDs, namely molecular and polymeric, including a modular approach to their synthesis, the ability to utilize a greater range of luminescent chromophores, and most importantly the ability to control the electronic and processing properties independently. Dendrimers consist of three components: the surface groups, the dendrons and the cores. The number of levels of branching points in the dendrons gives the generation number (G) of the dendrimer.

Electroluminescent dendrimers fall into two classes, those in which the dendrimer is fully conjugated[1−3] and those where the electroactive chromophores are connected by insulating dendrons.[4] The advantage of the former dendrimer type is that the conjugation provides a rigid framework for the dendrimer, which enables structure−property relationships to be more easily understood. For the dendrimers containing conjugated dendrons, both fluorescent[1,2] and phosphorescent[3] materials have been reported. The type of linking within the dendrons differentiates the three classes of conjugated dendrimers reported as the light-emitting component in an OLED. The dendrons have been mainly comprised of stilbene[2] or diphenylacetylene[1] moieties, and of these, the dendrimers containing stilbene units have been most widely studied. With the dendrimers that contain stilbene dendrons, it has been shown that the three-dimensional shape of the dendrimer plays a critical role in controlling the optoelectronic and device properties of the dendrimer. The size of the dendrimer increases with generation number, providing a molecular scale control of the spacing and hence interactions between the cores of neighboring dendrimers in solid films.[5] Intermolecular interactions are known to have a strong effect on the photophysics of conjugated molecules and polymers and can lead to the formation of excited states such as excimers or physical dimers and higher aggregates with an associated ground-state absorption.[6−10] An understanding of the impact of such interactions on light emission is important for the development of materials for OLEDs, and the control of intermolecular interactions afforded by changing generation provides a new tool with which to explore this issue.

[†] University of Durham.
[‡] Oxford University.
[§] University of St. Andrews.

10.1021/ma011996g CCC: $22.00
Published on Web 09/05/2002

Scheme 1[a]

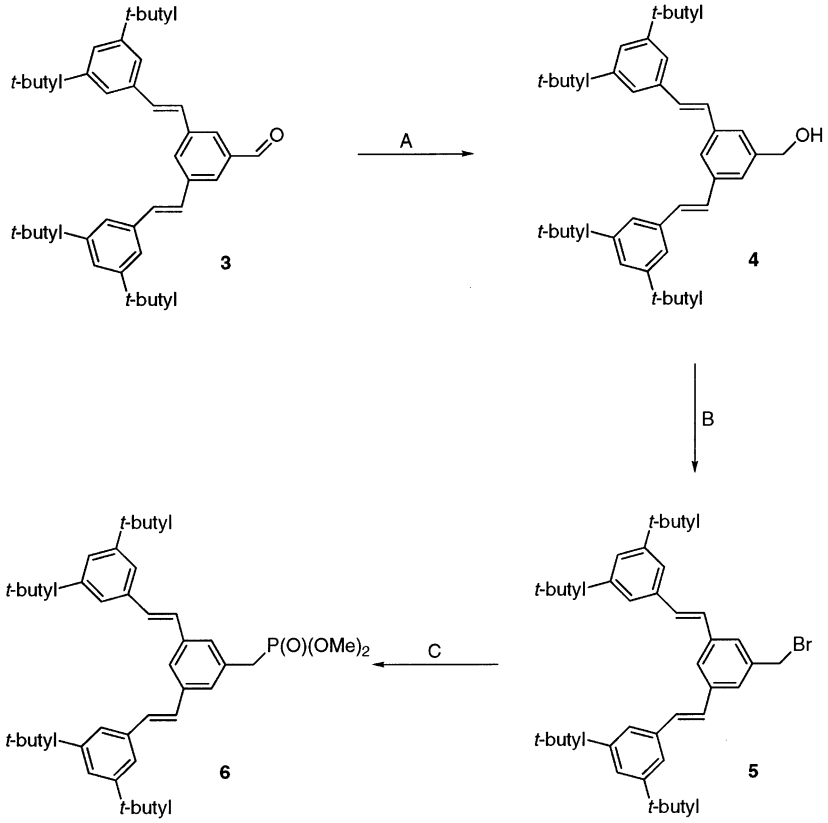

[a] Key: (A) sodium borohydride, tetrahydrofuran; (B) phosphorus tribromide, dichloromethane, room temperature, Ar; (C) trimethyl phosphite, heat.

Scheme 2[a]

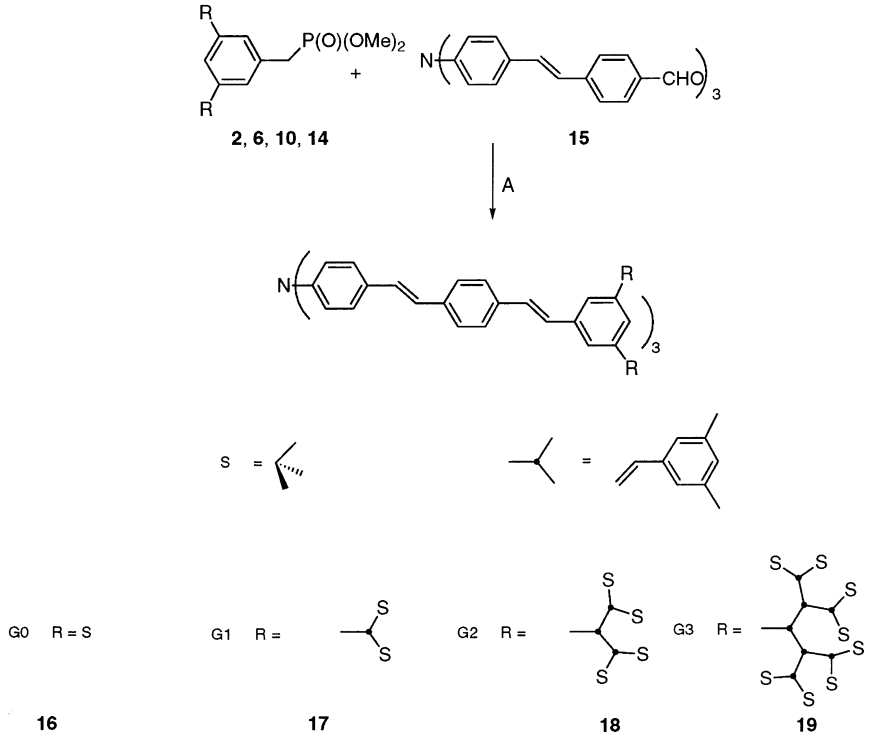

[a] Key: (A) potassium *tert*-butoxide, tetrahydrofuran, Ar.

We have previously reported the impact of generation on charge transport in a family of dendrimers containing tris(distyrylbenzenyl)amine cores, stilbene dendrons, and *tert*-butyl surface groups (Scheme 2).[5] By having a core which was known to be hole transporting, it was possible to directly measure the relationship between charge transport and core−core interactions in a controlled fashion at the molecular level. The hydrodynamic radii of the dendrimers were measured by gel-permeation chromatography and found to increase with

generation. This results in an increase in the separation between the cores of individual dendrimers leading to a distinctive scaling of the mobility with molecular size characteristic of hopping transport.[5] In addition, quantum chemical calculations have shown that although the dendrimers are fully conjugated, the electron delocalization is broken between the core and the dendrons by the *meta*-linking arrangement.[11] However, strong electronic coherences exist between the individual distyrylbenzene units within the core.

In this paper, we extend our study on understanding the intermolecular interactions in this family of dendrimers by exploring the nature of the light-emitting excited state and how it is affected by intermolecular interactions. In addition, we describe the strategy for the synthesis of the four generations of dendrimers and discuss the effect of generation on the redox properties of the dendrimers.

Results and Discussion

Synthesis. There have been a number of methods described for the formation of dendrimers containing stilbene dendrons.[12,13] The methodology used for the synthesis of the tris(distyrylbenzenyl)amine-cored electroluminescent dendrimers is illustrated in Schemes 1 and 2. The strategy is different to that of our earlier report for the preparation of luminescent dendrimers with stilbene dendrons. In that report we utilized an aldehyde moiety at the focus of the dendron to react with bis(phosphonate) derivatives for the formation of distyrylbenzene- and distyrylanthracene-cored dendrimers.[13] In this work we prepared the dendrimers from dendrons that contained benzylphosphonate foci and a "core" unit that contained the aldehyde functionality. The reason for this latter approach was that the required core unit with three phosphonates was expected to be more difficult to handle. The chemistry for the formation of the four dendron generations containing benzylphosphonate foci was the same and is illustrated for the first generation in Scheme 1. For the first to third generation aldehyde-focused dendrons, the aldehyde was reduced to the alcohol with sodium borohydride, brominated with phosphorus tribromide, and finally converted to the phosphonate using trimethyl phosphite. For the zeroeth generation dendron the synthesis of the phosphonate started from the corresponding bromide. The aldehyde focused dendrons were prepared by the literature procedure.[13] The terminology that we use for each of the dendron intermediates are [G-*X*]CHO, [G-*X*]CH_2OH, [G-*X*]CH_2Br, and [G-*X*]CH_2P, where *X* is the generation number and the suffix of the bracket describes the functionality at the foci, that is, aldehyde, benzyl alcohol, benzyl bromide, and benzylphosphonate, respectively. For all the dendron generations the yields of the reactions were moderate to excellent. The preparation of [G-0]CH_2P (**2**) was straightforward and was formed in an 89% yield from [G-0]CH_2Br (**1**).[14] For the first generation [G-1]CHO (**3**) was reduced to [G-1]CH_2OH (**4**), which was then brominated to give [G-1]CH_2Br (**5**), which was then reacted with trimethyl phosphite to give [G-1]CH_2P (**6**) in yields of 87%, 85%, and 91% respectively. For the second generation sequence, the yields were 97%, 56%, and 78% for the reduction of [G-2]CHO (**7**) to [G-2]CH_2OH (**8**), bromination of **8** to [G-2]CH_2Br (**9**), and phosphonation of **9** to [G-2]CH_2P (**10**). Finally, for the third generation starting with [G-3]CHO (**11**), the reduction, bromination, and phosphonation sequence went in yields of 80%, 47%, and 74% to give [G-3]CH_2OH (**12**), [G-3]CH_2Br (**13**), and [G-3]CH_2P (**14**), respectively. Of the three steps, the bromination occasionally proved capricious, particularly for the higher generations. We postulate that the lower yields of the desired benzyl bromides was due to the formation of a tris(dendronphosphite) byproduct, which was formed from a simple substitution of the phosphorus tribromide by the benzyl alcohols.

The synthesis of the tris(4-(4′-formylstyryl)phenyl)-amine (**15**) required for the formation of the cores of the dendrons was straightforward. Tris(4-bromophenyl)-amine[15] was reacted with 4-vinylbenzaldehyde using palladium catalysis to give tris(4-(4′-formylstyryl)-phenyl)amine **15** in a 53% yield.

With both the dendrons and central unit in hand, all that remained was to couple the dendrons and cores. The same general reaction conditions were used for each generation and involved using potassium *tert*-butoxide as the base and tetrahydrofuran as the solvent. In the case of the zeroeth to second generations, the reaction was carried out at room temperature while for the third generation the reaction was performed at reflux. Using these conditions the zereoth (**16**), first (**17**), second (**18**), and third (**19**) (denoted $[G\text{-}0]_3N$, $[G\text{-}1]_3N$, $[G\text{-}2]_3N$, and $[G\text{-}3]_3N$, respectively) amine-centered dendrimers were formed in the excellent yields of 86%, 81%, 76%, and 63% respectively. The zeroeth to second generation dendrimers were relatively easily purified by column chromatography over silica. The third generation was more difficult to purify by the same method, and only a small amount could be isolated directly from the reaction mixture. However, after treatment with iodine in toluene heated at reflux and careful chromatography over silica, the desired dendrimer could be isolated in good yield, suggesting that the impurities, at least in part, arose from geometrical isomers. With their high degree of symmetry, the assignment of the dendrimer structures by ^1H NMR was relatively straightforward up to the second generation. However, with the third generation, the number of overlapping resonances was such that only regions of the signals could be identified by analogy with the lower generations. The dendrimers were monodisperse by gel-permeation chromatography (GPC) against polystyrene standards and the structures were confirmed by mass spectrometry.

Electrochemistry. The redox properties of the dendrimers were studied by cyclic voltammetry and the cyclic voltammagrams are shown in Figure 1 with the $E_{1/2}$ potentials of the quasi-reversible redox processes shown in Table 1. The potentials are quoted against the ferrocenium/ferrocene couple. For the oxidation processes dichloromethane was determined to be the solvent of choice while for the reduction studies tetrahydrofuran was used. For the zeroeth generation dendrimer **16** two quasi-reversible oxidations, at 0.27 and 0.68 V, and one quasi-reversible reduction, at −2.62 V, were observed. The difference in the $E_{1/2}$ potentials for the first oxidation and the reduction was 2.89 V and this energy gap corresponds to light with a wavelength of 429 nm. This is close to the peak energy of the first absorption maxima in the UV−visible spectrum, which is at 421 nm (see Figure 2). One method of estimating the HOMO−LUMO energy gap of a material is to determine the energy corresponding to the onset of visible absorption. For **16**, the onset of visible absorption was at 471 nm (2.63 eV), and this is equal to the difference in

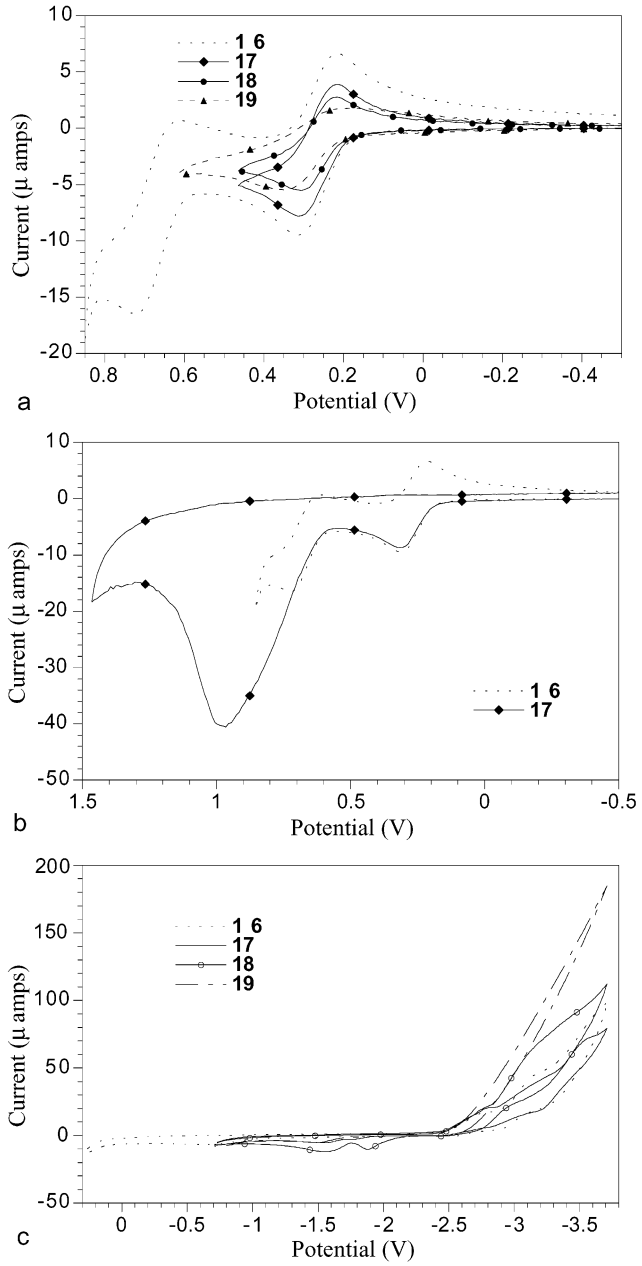

Figure 1. (a) Oxidation cyclic voltammagrams of **16**−**19** (concentration 1 mM, scan rate 100 mV/s). (b) Oxidation cyclic voltammagrams of **16** and **17** showing the chemically irreversible oxidation of **17** at more positive potentials (concentration 1 mM, scan rate 100 mV/s). (c) Reduction cyclic voltammagrams of **16**−**19** (concentration 1 mM, scan rate 100 mV/s).

Table 1. Reduction and Oxidation Potentials Found in the Cyclic Voltammetry Studies[a]

compound	concn/mM	type[b]	E_{pa}/V	E_{pc}/V	$E_{1/2}$/V
16	1	r	−2.49	−2.74	−2.62
	1	o1	0.32	0.22	0.27
	1	o2	0.73	0.62	0.68
17	1	o1	0.32	0.22	0.27
18	1	o1	0.31	0.22	0.27
19	1	o1	0.35	0.20	0.27

[a] Scan rate = 100 mV/s. [b] Key: r, reduction peak; o1, first oxidation peak; o2, second oxidation peak; E_{pa}, peak anodic potential; E_{pc}, peak cathodic potential.

potential between the onset of the reduction and first oxidation processes. The behavior of **16** on reduction was particularly sensitive to switching potential. When the switching potential was −2.80 V then the quasi-reversible reduction was observed. However, on moving the switching potential to −3.71 V more reduction processes were observed (Figure 1b). It was not possible to assign the $E_{1/2}$s due to the broad and overlapping nature of the processes and the fact that the oxidations of the reduced species were not electrochemically quasi-reversible. We believe that the complicated nature of the cyclic voltammagrams arises from the zeroeth generation dendrimer forming aggregates once reduced. As a consequence of the aggregation, we observe anodic peaks corresponding to the normal oxidation of the reduced species but with less current than would be expected and in addition we see two further smaller anodic peaks at −1.47 V and around −0.71 V which we ascribe to the aggregates. The complex cyclic voltammagrams are not due to chemically irreversible processes, as we are able to do repeated scans with no change in current.

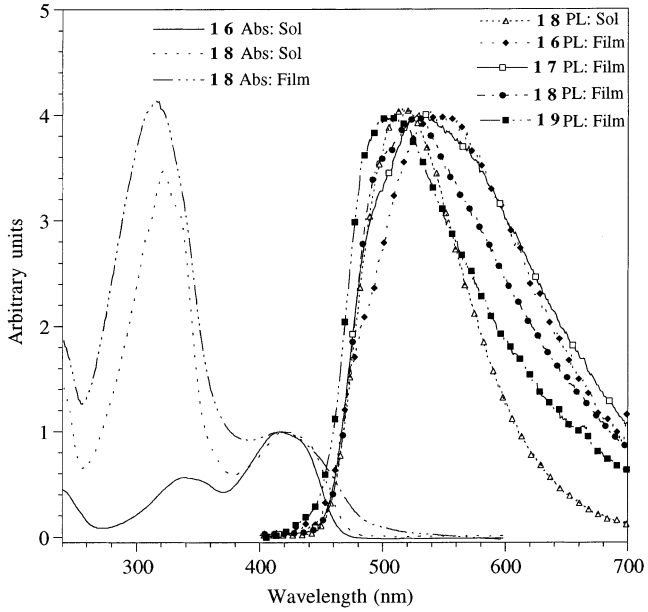

Figure 2. UV−visible absorption (Abs) and photoluminescence (PL) spectra.

On moving from the zereoth (**16**) to the first through to the third generation, **17**−**19**, dendrimers there was a significant change in the oxidation processes observed. For **17**−**19**, we observed one chemically quasi-reversible oxidation for each generation that is at the same $E_{1/2}$ (Table 1) as for the first oxidation of **16**. This shows that the *meta* arrangement of the dendron branching points breaks the delocalization pathway, so that the dendrons and core can be considered as being comprised of discrete electroactive units. However, the second core oxidation, which is observable for **16**, is not seen clearly for the higher generations. The second core oxidation for the higher generations is obscured by a chemically irreversible oxidation that occurs at a similar potential (Figure 1b). We assign the chemically irreversible oxidation to that of the stilbene dendrons. Evidence for this comes from the fact that for increasing generation the current associated with the chemically irreversible oxidation increases in proportion to the number of stilbene units in the dendron when compared with the current associated with the first core oxidation. At the concentrations used in the electrochemical experiments, we observed no aggregation phenomena of the oxidized species. A final observation we made was that the

separation of the oxidation (E_{pa}) and reduction (E_{pc}) peaks of the first oxidation process for the zeroeth to second generation were around 100 mV so the oxidations can be considered as quasi-reversible. However, for the third generation the difference between E_{pa} and E_{pc} for the oxidation process was 150 mV, which is a 50% increase on that observed for the lower generations (Figure 1a) The fact that the difference in E_{pa} and E_{pc} is the same for the zeroeth to second generation indicates that the availability of the core to heterogeneous electron transfer from the electrode is essentially equivalent. This is consistent with the relatively open structure imparted by the amine center and the relatively poor shielding of the core by the lower generation dendrons. For the third generation, the dendrons do hold the core further from the electrode slowing heterogeneous electron transfer.[16] In addition, in going from the zeroeth to third generation dendrimers, the peak currents were seen to decrease. The peak currents in linear sweep voltammetry and hence cyclic voltammetry are dependent on the diffusion coefficient of the substrate in solution. With increasing size of the dendrimers in going from the zeroeth to third generation, the diffusion coefficient would be expected to decrease, thus giving rise to the observed decrease in peak current. It is important to note that in the solid state the effect of the dendrons on the core−core interactions will be doubled when compared to the electrochemical experiments and this is confirmed by hole mobility measurements which show a decrease in hole mobility with increasing generation.[5] Also as discussed in the next section the control over core−core interactions plays an important role in understanding the optical properties of this dendrimer family.

The reduction cyclic voltammograms for the first to third generation dendrimers are shown in Figure 1c. For the first and second generation, we again observe several overlapping reductions and aggregation of the reduced species, giving rise to chemically reversible but not electrochemically quasi-reversible processes. For the third generation we do not see any defined reduction processes suggesting that the heterogeneous electron transfer from the electrode has been slowed. This is consistent with the oxidation of the third generation dendrimer.

Optical Properties. There has previously been little work on the nature of the excited state in dendrimers[17−20] and the only report of time-resolved luminescence on dendrimer films focused mainly on their subpicosecond dynamics.[17] Due to the current interest in dendrimers as light-emitting materials in OLEDs, a close understanding of the excited state in dendrimers is important, as is the level of control that the dendrimer generation can exert on the emission properties. We have used time-resolved luminescence spectroscopy in combination with photoluminescence quantum yield measurements to investigate the nature of the excited state of the tris(distyrylbenzenyl)amine-cored dendrimers. We compare solutions with films of different dendrimer generations to elucidate the important role of intermolecular interactions. The results suggest that an intermolecular excitation forms in films and is far more pronounced in low dendrimer generations.

The UV−visible absorption spectra of the amine centered dendrimers have been reported in detail elsewhere.[5,16] Figure 2 shows the UV−visible absorption spectra of the zeroeth generation dendrimer **16** in solution and the second generation dendrimer **18** in solution and film. There are three points to note; first, in going from solution to film the absorption spectra are essentially the same with regard to the onset of absorption and the peak maxima. Second, the attachment of the conjugated dendron to the tris(distyrylbenzenyl)-amine-cored dendrimers does not significantly red-shift the absorption edge of the dendrimers indicating that the *meta* linking arrangement at the first phenyl branching point to a first approximation breaks the delocalization pathway. The effect of the *meta* linking arrangement in the UV−visible spectra is consistent with the results from the electrochemical analysis. Finally, the first to third generation, **17**−**19**, dendrimers contain two components to their absorption spectra with maxima at 323 and 423 nm, which correspond to the absorption of the dendrons and core, respectively. The solution photoluminescence (PL) spectra of the four dendrimers are all the same as that of the second generation **18** shown in Figure 2. Solutions of the dendrimers give strong green luminescence, and the solution PLQYs of the zeroeth, first, second, and third generation dendrimers were 0.61, 0.63, 0.63, and 0.62, respectively. The error in each solution PLQY measurement was ±0.1. Time-resolved luminescence measurements showed a monoexponential decay with a lifetime of 1.8 ± 0.1 ns for all dendrimer generations (see Figures 3−6)

In the solid state, the steady-state PL spectra, photoluminescence quantum yield (PLQY), and time-resolved luminescence are very different from the solution results. The steady-state PL spectra (Figure 2) show a substantial red tail that is most pronounced in the zeroeth **16** and first **17** generations, and weaker in the second generation **18** dendrimer. This red tail is further reduced in the third generation **19** to the extent that the PL spectrum for this material is much closer to that of a dilute solution.[21] A striking difference between solution and film is in PLQY: the film PLQY is up to an order of magnitude smaller than in solution. The film PLQYs are shown in Table 2, and it can be seen that there is an increase in PLQY with increasing generation number. For each generation, PLQYs following excitation at 325 nm (in the dendron band) and 442 nm (in the core) were the same within the experimental errors.

The time-resolved PL of the films are shown in Figures 3−6, and summarized in Table 2. The behavior is much more complicated than for solution, and in general three exponentials are required to fit the measured decays. The decays depend strongly on the detection wavelength and to illustrate this we show data for emission at 480 nm (on the blue side of the spectrum) and 600 nm (corresponding to the red shoulder). This behavior can be seen for the zeroeth generation **16** in Figure 3: the film emission at 480 nm has a rapid nonexponential decay, which is much faster than the solution PL decay. At 600 nm the decay is initially faster than in solution, but has a longer-lived component which dominates at longer time, causing the film decay curve to cross the solution decay.

The results of time-resolved PL measurements of the higher generations, **17**−**19**, are shown in Figures 4−6. It is again found that for a detection wavelength of 480 nm, the film decay is much faster than in solution. For **18** and **19**, it is also found that the PL decay at 600 nm is longer lived than at 480 nm. However, the difference is smaller than for the zeroeth generation.

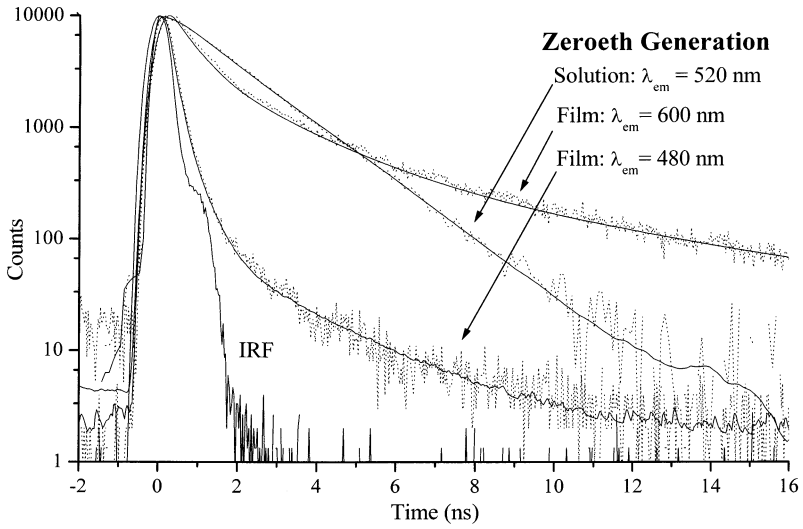

Figure 3. Time-resolved luminescence of the zeroeth generation dendrimer **16**. IRF is the instrumental response function. Dotted lines represent the raw data and solid lines the fitted function.

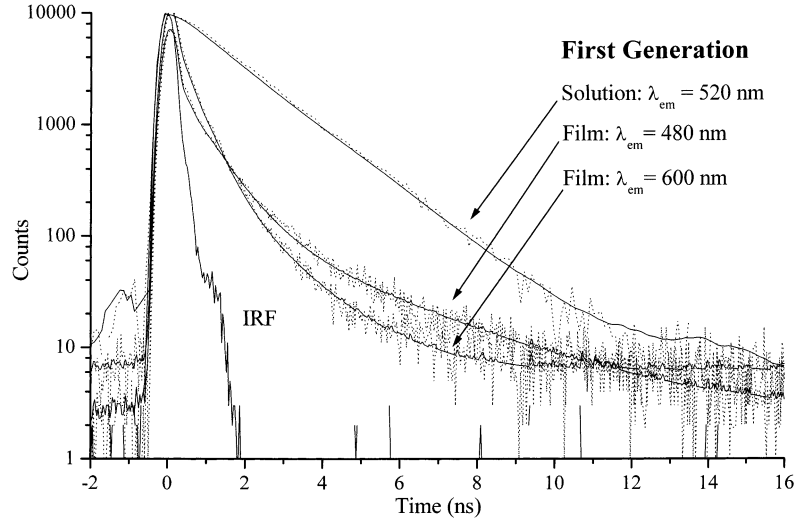

Figure 4. Time-resolved luminescence of the first generation dendrimer **17**. IRF is the instrumental response function. Dotted lines represent the raw data and solid lines the fitted function.

The main observations in solution are that the spectrum, time dependence of the PL, and PLQYs are the same for all generations. These three results very strongly imply that in solution the same excited state is responsible for the emission in all generations. With a measured lifetime of 1.8 ± 0.1 ns and quantum yield of 0.62 ± 0.1 the natural radiative lifetime of the excited state can be estimated to be 2.9 ± 0.5 ns for all generations. This value is characteristic of a fully allowed transition and taking account of the spectra, we assign the solution PL to emission from a singlet excited state on the core of the dendrimer. We note in passing that much faster processes such as energy transfer from the dendron to the core[17,18] lie outside the time resolution of our experiments.

A comparison of the film absorption spectra with what has been observed for solutions,[22] shows that the bands of the film are somewhat broader. In films there are a variety of different molecular conformations, which will result in a distribution of interaction energies and inhomogeneous broadening of the electronic transition. Furthermore, close packing of the dendrimer units in films may result in a weak interaction between ground states. Interestingly though, except for a weak Davydov type of splitting, the core absorption remains unaffected by the dendrimer generation as has been observed in solutions. This has previously led to the suggestion that electronic interactions between dendrons and the core do not perturb the core and that consequently an exciton is localized on the core after equilibration.[23] This situation seems to prevail in films as well.

The difference between the PL spectra of the dendrimers in solution and films can be substantial.[21] The film PL spectrum of the zereoth generation dendrimer **16** undergoes the most dramatic change compared with the solution spectrum with the appearance of a pronounced red shoulder. The red shoulder was found to decrease with increasing dendrimer generation. This suggests that the origin of this red shoulder is core−core interactions which accordingly are strongest in the zeroeth generation.

Intermolecular interactions such as excimers and aggregates can lead to red-shifted emission and reduced PLQY.[24] The latter can be caused by transfer of the excitation to quenching and defect sites, a situation that is more likely to occur in films than solution due to the

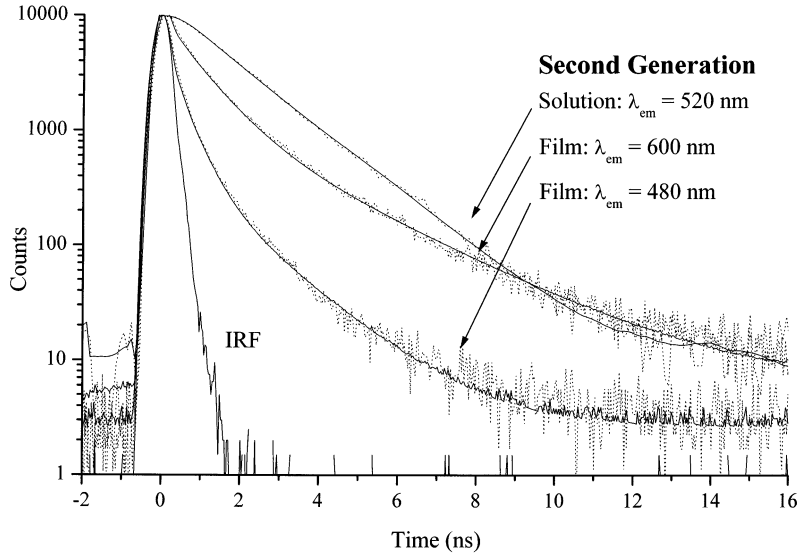

Figure 5. Time-resolved luminescence of the second generation dendrimer **18**. IRF is the instrumental response function. Dotted lines represent the raw data and solid lines the fitted function.

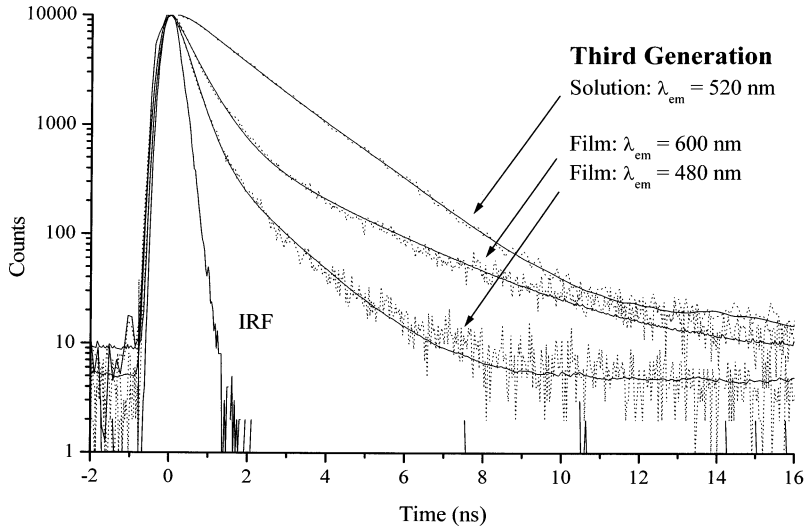

Figure 6. Time-resolved luminescence of the third generation dendrimer **19**. IRF is the instrumental response function. Dotted lines represent the raw data and solid lines the fitted function.

Table 2. Summary of the Time-resolved Luminescence Data for Films of the Four Dendrimer Generations[a]

	$\lambda_{det} = 480$ nm		$\lambda_{det} = 480$ nm		$\lambda_{det} = 480$ nm		$\lambda_{det} = 600$ nm		$\lambda_{det} = 600$ nm		$\lambda_{det} = 600$ nm		
C	τ_1 (ns)	A_1	τ_2 (ns)	A_2	τ_3 (ns)	A_3	τ_1 (ns)	A_1	τ_2 (ns)	A_2	τ_3 (ns)	A_3	ϕ (%)
16	0.06	0.959	0.39	0.040	2.3	0.001	0.48	0.740	1.9	0.230	7.5	0.030	5
17	< 0.05	0.950	0.45	0.047	1.4	0.003	<0.05	0.985	0.75	0.014	3.0	0.001	7
18	< 0.05	0.970	0.45	0.025	1.5	0.005	<0.05	0.948	0.81	0.040	2.4	0.002	8
19	0.32	0.840	0.83	0.150	3.0	0.010			0.50	0.507	2.0	0.493	12

[a] **C** stands for the compound. A_n denotes the amplitude of the nth component of the fitted decay. ϕ denotes the PLQY of the film following excitation at 325 nm. The error of the PLQY data is ±10% of the stated value. For **17** and **18**, the fast component is ill-defined due to the time resolution of the experiment.

relatively dense packing of dendrimer units. This is consistent with the much-reduced PLQY in films compared to the solutions. Furthermore, the zeroeth generation **16** (where core−core interaction could be strongest) has the lowest PLQY and largest red-shift in the steady-state PL at room temperature,[21] which is consistent with this picture. We note, however, that the high energy side of the PL spectrum is similar to that in solution, showing that there is also a substantial contribution from intramolecular singlet excited states.

The key features of the film time-resolved luminescence that require explanation are the more complicated decay profile, including long-lived components, the much slower decay at longer wavelength, and the effect of generation. Like the steady-state spectra, these observations can be explained by the emission being a superposition of intramolecular singlets and an intermolecular excited state. The long-lived component is much more pronounced in the zeroeth generation **16** than in the higher generations, and this can be understood to be due to stronger core−core interactions in this

material because of the absence of dendrons. We propose that the fast components of the film PL decay are due to migration of excitations to quenching sites and formation of the intermolecular excitations. Finally we consider the nature of the intermolecular excitation. This could be an excimer, physical dimer or higher aggregate. It is not easy to distinguish between these possibilities, but as there is no evidence for ground state absorption associated with an aggregate (or dimer), we believe it is more likely that the intermolecular excitation is an excimer.

Conclusion

We have demonstrated that dendrimers containing tris(distyrylbenzenyl)amine cores, stilbene dendrons, and *tert*-butyl surface groups can be formed in good yields from phosphonate focused dendrons and a unit containing three aldehyde moieties. Electrochemical analysis indicated that the dendrimer generation had a strong effect on the redox processes. The PLQY and time-resolved luminescence measurements show that the dendrimer generation has a strong effect on the photophysics of films which can be understood to arise from changing the extent of intermolecular interactions. The dendrimer generation therefore provides a powerful and systematic way of controlling these interactions.

Experimental Section

Measurements. NMR spectra were recorded on a Bruker DPX 400 MHz or an AMX 500 MHz spectrometer: sp = surface phenyl; cp = core phenyl; cv = core vinyl; bp = branch phenyl. All *J* values are in hertz. IR spectra were recorded on a Perkin-Elmer 1000 infrared spectrometer, and all spectra were recorded either as a solution in spectroscopic grade chloroform or as a KBr disk. UV−visible spectra were recorded on a Perkin-Elmer UV−visible Lambda 14P spectrometer and were recorded as a solution in spectroscopic grade chloroform, dichloromethane, or ethanol. Mass spectra were recorded on a Hewlett-Packard 1050 atmospheric pressure chemical ionization mass spectrometer (APCI) (+ve mode), a VG Autospec for CI and FAB, or a Micromass TofSpec 2E for matrix-assisted laser desorption/ionization-time-of-flight (MALDI−TOF) from dithranol in reflectron mode. Melting points were recorded on a Gallenkamp melting point apparatus and are uncorrected. Microanalyses were carried out in the Inorganic Chemistry Laboratory, University of Oxford, Oxford, U.K. Gel permeation chromatography was carried out using PLgel μm Mixed-A columns (600 mm + 300 mm lengths, 7.5 mm diameter) from Polymer Laboratories calibrated with polystyrene narrow standards (M_p = 1300 to 15.4 × 10^6) in tetrahydrofuran with toluene as flow marker. The tetrahydrofuran was degassed with helium and pumped with a rate of 1 mL/min at 30.0 °C. Light petroleum refers to the fraction of boiling point 60−80 °C, unless otherwise stated, and ether refers to diethyl ether. When solvent mixtures are used for chromatography over silica the proportions are given by volume.

Electrochemistry was performed using an EG&G Princeton Applied Research potentiostat/galvanostat model 263A. All measurements were made at room temperature on samples dissolved in freshly distilled dichloromethane or tetrahydrofuran, with 0.1 M tetra-*n*-butylammonium hexafluorophosphate as the electrolyte. The tetrahydrofuran was distilled from sodium wire and benzophenone under argon, and then distilled from lithium aluminum hydride under argon. Dichloromethane was purified by the literature procedure and then freshly distilled from calcium hydride.[25] The electrolyte was purified by recrystallization from ethanol. The solutions were deoxygenated with argon. A glassy carbon working electrode, platinum wire counter electrode, and Ag/3 M NaCl/AgCl(sat) reference electrode was used. The ferrocenium/ferrocene couple was used as standard,[26] and the ferrocene was purified by sublimation. In all cases several scans were carried out to confirm the chemical reversibility of the redox processes.

Solution photoluminescence quantum yields (PLQYs) were measured by a relative method using quinine sulfate in 0.5 M Sulfuric acid at room temperature as a standard.[27] The dendrimers were dissolved in tetrahydrofuran (THF) and freeze−thaw degassed. Photoluminescence spectra were recorded in a JY Horiba Fluoromax 2 fluorimeter, with the dendrimer solutions excited at 320 nm. The optical densities of the standard and sample were similar and small (less than/equal to 0.1). The accuracy of these measurements is estimated to be ±10%.

Films were spin-coated from a THF solution with a dendrimer concentration of 10 mg/mL at 1000 rpm for 1 min to give a thickness of about 150 nm. Their PLQY were measured using an integrating sphere in accordance with Greenham et al.[28] using a helium cadmium laser (Kimmon) as the excitation source. The excitation intensity was 0.2 mW at 325 nm and 0.3 mW at 442 nm, and the measurements were performed under a nitrogen atmosphere.

Time-resolved luminescence measurements were made by the time-correlated single-photon-counting technique and films were mounted in a sample chamber which was evacuated to a pressure of ∼10^{-2} mbar during the experiment. The excitation source was provided by a pulsed light-emitting diode system (Picoquant PLS 370). The excitation wavelength was 380 nm, and the temporal width of the excitation pulses (fwhm) was approximately 350 ps at a repetition rate of 20 MHz. The energy per pulse was in the order of picojoules. The detection system consisted of a cooled 6 μm Hamamatsu micro channel plate photomultiplier tube (RU-3809U-50), and the detection wavelength was selected by a f = 3 monochromator with an entrance slit corresponding to a resolution of 8 nm. The instrumental response function of the experiment had a fwhm of ∼400 ps. The time-resolved data were analyzed using a least squares routine based upon the Marquardt−Levenberg algorithm. The data were fitted to a sum of exponentials deconvoluting the decay from the instrumental response function. The quality of the fit was determined by the sum of the χ^2 parameter (whereby a perfect fit gives χ^2 = 1) and a visual inspection of the residuals.

[G-1]CH_2OH, 4. A mixture of [G-1]CHO, **3** (3.00 g, 6.61 mmol), and sodium borohydride (840 mg, 22.2 mmol) in tetrahydrofuran (150 mL) was heated at reflux for 110 min. The solvent was then completely removed and light petroleum (30−40) and aqueous hydrochloric acid (3 M, 30 mL) were added and stirred until effervescence had ceased. The white precipitate was then filtered and dried under vacuum leaving **4** (2.63 g, 87%). A sample for analysis was recrystallized from a dichloromethane−light petroleum mixture, mp 226−228 °C. Anal. Calcd for $C_{39}H_{52}O$: C, 87.3; H, 9.8. Found: C, 87.3; H, 9.5. ν_{max}($CHCl_3$)/cm^{-1}: 3608 (OH), 1596 (C=C), and 964 (C=C−H trans). λ_{max}(CH_2Cl_2)/nm: 307 (log ϵ/dm^3 mol^{-1} cm^{-1} 4.80), 312 (4.80), 315 (4.80), and 330 sh (4.66). δ_H(400 MHz; $CDCl_3$): 1.41 (36 H, s, *t*-Bu), 1.81 (1 H, t, J = 6, OH), 4.79 (2 H, d, J = 6, CH_2O), 7.17 and 7.28 (4 H, d, J = 16, G1-vinyl H), 7.41 (2 H, dd, J = 1.5, sp H), 7.43 (4 H, d, J = 1.5, sp H), 7.49 (2 H, bs, cp H), and 7.66 (1 H, s, cp H). m/z (APCI$^+$) 519.3 [(M − OH)$^+$, 100%).

[G-2]CH_2OH, 8. A mixture of [G-2]CHO, **7** (2.52 g, 2.16 mmol), and sodium borohydride (164 mg, 4.34 mmol) in tetrahydrofuran (75 mL) was heated at reflux for 40 min. Water (50 mL) and dichloromethane (100 mL) were added. The aqueous layer was separated and extracted with dichloromethane (2 × 30 mL). The combined organic layers were washed with water (100 mL) and brine (100 mL), dried over anhydrous sodium sulfate and filtered and the solvent removed to leave a white solid. The residue was purified by column chromatography over silica using dichloromethane as eluent to give **8** (2.43 g, 97%) as a white solid, mp 310 °C. Anal. Calcd for $C_{87}H_{108}O$: C, 89.3; H, 9.3. Found: C, 89.4; H, 9.3. ν_{max}(KBr disk)/cm^{-1}: 3567 (OH), 1595 (C=C), and 961 (C=C−H trans). λ_{max}(CH_2Cl_2)/nm: 322 (log ϵ/dm^3 mol^{-1} cm^{-1} 5.43) and 330 sh (5.34). δ_H(400 MHz, $CDCl_3$): 1.41 (72 H, s, *t*-Bu), 1.78 (1 H, t, J = 6, OH), 4.82 (2 H, d, J = 6, CH_2O), 7.19 and 7.30 (4 H, d,

J = 16.5, G-2 vinyl H), 7.30 (4 H, s, G-1 vinyl H), 7.40 (4 H, dd, J = 1.5, sp H), 7.45 (8 H, d, J = 1.5, sp H), 7.53 (2 H, br s, cp H), 7.65 (6 H, br s, bp H), and 7.71 (1 H, br s, cp H). *m/z* (FAB): 1169.6 (M^+, 100%).

[G-3]CH_2OH, 12. Sodium borohydride (121 mg, 3.20 mmol) was added to a solution of [G-3]CHO, **11** (3.85 g, 1.59 mmol), in tetrahydrofuran (50 mL), and the reaction mixture was heated at reflux for 135 min. The solvent was then removed, dichloromethane (50 mL) was added, and the solution was washed with water (50 mL) and brine (50 mL), dried over anhydrous sodium sulfate, and filtered and the solvent removed to leave a yellow foam. The residue was purified by column chromatography over silica using a dichloromethane−light petroleum mixture (2:3) and then recrystallization from a dichloromethane−methanol mixture to give **12** (3.07 g, 80%) as a yellow powder, mp 248 °C. Anal. Calcd for $C_{183}H_{220}O$: C, 90.2; H, 9.1. Found: C, 89.9; H, 8.9. ν_{max} (KBr disk)/cm^{-1}: 3569 (OH), 1594 (C═C), and 959 (C═C−H trans). λ_{max} (CH_2Cl_2)/nm: 323 (log ϵ/dm^3 mol^{-1} cm^{-1} 5.59) and 334 sh (5.52). δ_H(400 MHz; $CDCl_3$): 1.39 (144 H, s, *t*-Bu), 1.80 (1H, t, J = 6, OH), 4.85 (2 H, d, J = 6, CH_2O), 7.19 and 7.31 (16 H, d, J = 16, G-3 vinyl H), 7.32 (4 H, s, G-1 vinyl H), 7.34 (8 H, s, G-2 vinyl H), 7.39 (8 H, dd, J = 1.5, sp H), 7.44 (16 H, d, J = 1.5, sp H), 7.57 (2 H, br s, cp H), 7.67 (12 H, br s, G-2 bp H), 7.68 (4 H, br d, J = 1, G-1 bp H), 7.70 (1 H, br s, cp H), and 7.74 (2 H, br s, G-1 bp H). *m/z* (MALDI): 2434.94 (M^+, 100%).

[G-1]CH_2Br, 5. Phosphorus tribromide (2.8 mL, 30 mmol) was added to a solution of [G-1]CH_2OH, **4** (1.60 g, 3.0 mmol), in dichloromethane (50 mL), and the solution was stirred at room temperature for 3 h. Propan-2-ol (14 mL) was added slowly, and the solvent was completely removed. The residue was purified by column chromatography over silica using a dichloromethane−light petroleum mixture (40−60) (1:9) as eluent to give **5** (1.52 g, 85%). A sample for analysis was recrystallized from a dichloromethane−light petroleum mixture, mp 222−223 °C. Anal. Calcd for $C_{39}H_{51}Br$: C, 78.1; H, 8.6. Found: C, 77.75; H, 8.7. ν_{max}($CHCl_3$)/cm^{-1}: 1596 (C═C) and 964 (C═C−H trans). λ_{max}($CHCl_3$)/nm: 315 (log ϵ/dm^3 mol^{-1} cm^{-1} 4.82) and 333 sh (4.64). δ_H(400 MHz; $CDCl_3$): 1.38 (36 H, s, *t*-Bu), 4.55 (2 H, s, CH_2Br), 7.12 and 7.24 (4 H, d, J = 16, G-1 vinyl H), 7.39 (2 H, dd, J = 1.5, sp H), 7.40 (4 H, d, J = 1.5, sp H), 7.46 (2 H, d, J = 1, cp H), and 7.63 (1 H, br s, cp H). *m/z* (APCI$^+$): 521 ((M − Br)$^+$, 100%).

[G-2]CH_2Br, 9. A solution of [G-2]CH_2OH, **8** (2.43 g, 2.08 mmol), and phosphorus tribromide (2.0 mL) in dichloromethane (50 mL) were stirred at room temperature under argon for 46 h. Water (100 mL) was added carefully, and then dichloromethane (150 mL) was added. The organic layer was separated and washed with aqueous sodium bicarbonate solution (5% w/v, 100 mL), water (100 mL), and brine (2 × 100 mL), dried over anhydrous sodium sulfate, and filtered and the solvent removed. The residue was purified by column chromatography over silica using dichloromethane as eluent to give **9** (1.43 g, 56%) as a white solid, mp >250 °C dec. ν_{max}(KBr disk)/cm^{-1}: 1595 (C═C) and 961 (C═C−H trans). λ_{max}(CH_2Cl_2)/nm: 321 (log ϵ/dm^3 mol^{-1} cm^{-1} 5.34) and 333 sh (5.24). δ_H(500 MHz; $CDCl_3$): 1.41 (72 H, s, *t*-Bu), 4.59 (2 H, s, CH_2Br), 7.19 and 7.30 (8 H, d, J = 16.5, G-2 vinyl H), 7.28 (4 H, s, G-1 vinyl H), 7.40 (4 H, dd, J = 1.5, sp H), 7.44 (8 H, d, J = 1.5, sp H), 7.52 (2 H, d, J = 1, cp H), 7.64 (4 H, br s, bp H) 7.65 (2 H, br s, bp H), and 7.71 (1 H, br s, cp H). *m/z* (FAB): 1232.5 (M^+, 100%).

[G-3]CH_2Br, 13. Phosphorus tribromide (1.2 mL, 12.4 mmol) was added to [G-3]CH_2OH, **12** (3.01 g, 1.24 mmol), in dichloromethane (120 mL), and the yellow solution was stirred in the dark under argon for 6 days. Water (50 mL) was added carefully followed by ether (300 mL). The organic layer was separated and washed with water (100 mL) and brine (70 mL), dried over anhydrous sodium sulfate, filtered and the solvent removed. The residue was passed through a plug of silica using a dichloromethane−light petroleum mixture (2:3) as eluent to give **13** (1.45 g, 47%) as a white solid. A sample for analysis was recrystallized from a dichloromethane−methanol mixture, mp 256−258 °C. Anal. Calcd for $C_{183}H_{219}Br$: C, 88.0; H, 8.8. Found: C, 87.7; H 8.5. ν_{max} (KBr disk)/cm^{-1}: 1594 (C═C) and 960 (C═C−H trans). λ_{max} (CH_2Cl_2)/nm: 323 (log ϵ/dm^3 mol^{-1} cm^{-1} 5.54) and 334 sh (5.46). δ_H(400 MHz; $CDCl_3$): 1.39 (144 H, s, *t*-Bu), 4.63 (2 H, s, CH_2Br), 7.19 and 7.31 (16 H, d, J = 16, G-3 vinyl H), 7.30 (4 H, s, G-1 vinyl H), 7.34 (8 H, s, G-2 vinyl H), 7.39 (8 H, dd, J = 1.5, sp H), 7.44 (16 H, d, J = 1.5, sp H), 7.57 (2 H, br s, G-1 bp H), 7.67 (12 H, br s, G-2 bp H), 7.68 (4 H, br s, G-1 bp H), 7.70 (1 H, br s, cp H), and 7.74 (2 H, br s, cp H). *m/z* (MALDI): 2498.74 (M^+, 100%).

[G-0]CH_2P, 2. A mixture of [G-0]CH_2Br,[14] **1** (1.86 g, 6.57 mol), and trimethyl phosphite (7.6 mL, 64 mmol) was stirred at 95 °C for approximately 3 h, and then allowed to cool. The solution was diluted with ether (25 mL) and washed with water (6 × 25 mL), dried over anhydrous sodium sulfate, and filtered and the solvent removed to leave **2** (1.82 g, 89%) as a white solid, mp 55−56 °C. Anal. Calcd for $C_{17}H_{29}O_3P$: C, 65.4, H, 9.4. Found: C, 65.4; H, 9.2. ν_{max} ($CHCl_3$)/cm^{-1}: 1064 and 1032 (P−O−C). λ_{max}(ethanol)/nm: 256 sh (log ϵ/dm^3 mol^{-1} cm^{-1} 2.22), 264 (2.34), and 271 sh (2.25). δ_H(400 MHz; $CDCl_3$): 1.32 (18 H, s, *t*-Bu), 3.17 (2 H, d, J = 21.5, CH_2P), 3.65 (6 H, d, J = 11, OMe), 7.14 (2 H, dd, J = 2 and J = 2, 2-H and 6-H), and 7.31 (1 H, dd, J = 2 and J = 4, 4-H). δ_C(100.6 MHz; $CDCl_3$) 31.4, 33.2 (d, J = 137, CH_2P), 34.7, 52.8 (d, J = 7, POMe), 120.8 (d, J = 3, phenyl C), 124.08 (d, J = 7, phenyl C), 130.0 (d, J = 9, phenyl C), and 150.9(d, J = 3, phenyl C). *m/z* (APCI$^+$) 313.3 (MH^+, 100%).

[G-1]CH_2P, 6. A mixture of [G-1]CH_2Br, **5** (500 mg, 0.52 mmol), and trimethyl phosphite (5.0 mL, 38 mmol) was heated at 110 °C for 3 h. Methanol (100 mL) was added, and then water was slowly added until a precipitate formed. The precipitate was collected and dried under vacuum to give **6** (477 mg, 91%). A sample for analysis was recrystallized from a dichloromethane/methanol/water mixture, mp 207−208 °C. Anal. Calcd for $C_{41}H_{57}O_3P$: C, 78.3; H, 9.1. Found: C, 78.2; H, 9.4. ν_{max}($CHCl_3$)/cm^{-1}: 1596 (C═C), 1062 (P−O−C), 1038 (P−O−C), and 964 (C═C−H trans). λ_{max} ($CHCl_3$)/nm: 308 (log ϵ/dm^3 mol^{-1} cm^{-1} 4.75) 316 (4.75), and 331 sh (4.60). δ_H(400 MHz; $CDCl_3$): 1.38 (36 H, s, *t*-Bu), 3.23 (2 H, d, J = 21.5, CH_2P), 3.72 (6 H, d, J = 10.5, OMe), 7.12 and 7.23 (4 H, d, J = 16, G1 vinyl H), 7.38 (4 H, m, cp H and sp H), 7.40 (4 H, d, J = 1.5, sp H), 7.62 (1 H, br m, cp H). *m/z* (APCI$^+$): 630 (MH^+, 100%).

[G-2]CH_2P, 10. A mixture of [G-2]CH_2Br, **9** (1.24 g, 1.00 mmol), and trimethyl phosphite (10 mL) was heated at 100 °C under argon for 18 h. Excess trimethyl phosphite was removed by distillation under reduced pressure and the residue recrystallized from a dichloromethane−methanol mixture. The residue was collected and purified by column chromatography over silica using dichloromethane as eluent to give **10** (983 mg, 78%) as a white solid, mp >220 °C dec. Anal. Calcd for $C_{89}H_{113}O_3P$: C, 84.7; H, 9.0. Found: C, 84.6; H, 9.0. ν_{max}(KBr disk)/cm^{-1}: 1595 (C═C), 1056 and 1028 (P−O−C), and 958 (C═C−H trans). λ_{max}(CH_2Cl_2)/nm: 321 (log ϵ/dm^3 mol^{-1} cm^{-1} 5.24) and 335 sh (5.13). δ_H(400 MHz; $CDCl_3$): 1.40 (72 H, s, *t*-Bu), 3.26 (2 H, d, J = 21.5, CH_2P), 3.76 (6 H, d, J = 11, OMe), 7.19 and 7.30 (8 H, d, J = 16, G-2 vinyl H), 7.27 (4 H, s, G-1 vinyl H), 7.40 (4 H, br s, sp H), 7.44 (10 H, br s, cp H and sp H), 7.64 (6 H, bs, cp H and bp H), and 7.70 (1 H, br s, cp H). *m/z* (CI$^+$): 1261.8 (MH^+, 100%).

[G-3]CH_2P, 14. Trimethyl phosphite (5.4 mL, 46 mmol) was added to [G-3]CH_2Br, **13** (1.14 g, 0.455 mmol), and the suspension heated at 100 °C under argon for 2 h. Excess trimethyl phosphite was removed by distillation under reduced pressure and residue was recrystallized from a dichloromethane−methanol mixture. The residue was purified by column chromatography over silica using dichloromethane as eluent to give **14** (853 mg, 74%) as a white solid, mp 232 °C. Anal. Calcd for $C_{185}H_{225}O_3P$: C, 87.9; H, 9.0. Found: C, 87.3; H, 9.2. ν_{max}(KBr disk)/cm^{-1}: 1594 (C═C), 1059 and 1033 (P−O−C), and 960 (C═C−H trans). λ_{max}(CH_2Cl_2)/nm: 322 (log ϵ/dm^3 mol^{-1} cm^{-1} 5.59) and 334 sh (5.50). δ_H(400 MHz; $CDCl_3$): 1.39 (144 H, s, *t*-Bu), 3.29 (2 H, d, J = 21, CH_2P), 3.79 (6 H, d, J = 11, OMe), 7.19 and 7.31 (16 H, d, J = 16, G-3 vinyl H), 7.29 (4 H, s, G-1 vinyl H), 7.33 (8 H, s, G-2 vinyl H), 7.39 (8 H, dd, J = 1.5, sp H), 7.44 (16 H, d, J = 1.5, sp H), 7.48 (2 H, br m, G-1 cP H), 7.65−7.70 (17 H, cp and/or bp H), 7.67 (8 H, s, G-2 bp H), 7.67 (5 H, br s, cp H and G1 bp H),

7.73 (2 H, s, cp and or bp H). *m*/*z* (MALDI): 2527.8 (M^+, 100%) and 2590.7 (MCu^+, 97%).

Tris-4-(4-formylstyryl)phenylamine, 15. A mixture of tris(4-bromophenyl)amine[15] (6.34 g, 13.1 mmol), 4-vinylbenzaldehyde (6.95 g, 53 mmol), 2,6-di-*tert*-butyl-*p*-cresol (11.57 g, 0.053 mmol), sodium carbonate (5.57 g, 53 mmol), *trans*-di(*μ*-aceto)-bis[*o*-(di-*o*-tolylphosphino)benzyl]dipalladium(II) (37 mg, 39 *μ*mol), and *N*,*N*-dimethylacetamide (70 mL) was deoxygenated by alternate exposure to high vacuum and flushing with argon over 30 min. The mixture was heated at 130 °C under argon for 47 h and then allowed to cool. Aqueous hydrochloric acid (3 M, 10 mL) and chloroform (150 mL) were added. The organic layer was separated and washed with water (2 × 100 mL) and brine (100 mL), dried over anhydrous sodium sulfate, and filtered and the solvent removed to leave an orange residue. The residue was purified in two steps. First, the residue was recrystallized from a dichloromethane−light petroleum mixture and then the collected precipitate was purified by column chromatography over silica using a dichloromethane−ethyl acetate mixture (19:1) to give **15** (4.47 g, 53%), mp 256−258 °C. Anal. Calcd for $C_{45}H_{33}NO_3$: C, 85.0; H, 5.2; N, 2.2. Found: 84.8; H, 5.2; N, 2.2. ν_{max}(KBr disk)/cm^{-1}: 1691 (C═O) and 965 (C═C−H trans). $\lambda_{max}(CH_2Cl_2)$/nm: 316 (log ϵ/dm^3 mol^{-1} cm^{-1} 4.76) and 432 (4.99). δ_H(500 MHz, $CDCl_3$): 7.08 and 7.24 (6 H, d, J = 16.5, cv H), 7.15 and 7.48 (12 H, AA′BB′, cp H), 7.65 and 7.87 (12 H, AA′BB′, cp H), and 10.00 (3 H, s, CHO). *m*/*z* (FAB): 635.2 (M^+, 100%).

[G-0]$_3$N, 16. A mixture of [G-0]CH_2P, **2** (986 mg, 3.16 mmol), **15** (498 mg, 0.78 mmol), and potassium *tert*-butoxide (353 mg, 3.15 mmol) in tetrahydrofuran (80 mL) was stirred at room temperature under argon for approximately 16 h, giving a fluorescent yellow solution. Water (25 mL) and dichloromethane (175 mL) were added. The organic layer was separated, dried over anhydrous sodium sulfate, and filtered, and the solvent was removed to give a yellow solid. The residue was purified by column chromatography over silica using a dichloromethane−light petroleum mixture (1:4 to 1:0) to give **16** (804 mg, 86%) as a bright yellow solid, mp 182 °C. Anal. Calcd for $C_{90}H_{99}N$: C, 90.5; H, 8.4; N, 1.2. Found: C, 90.2; H, 8.2; N, 1.2. ν_{max}(KBr disk)/cm^{-1}: 957 (C═C−H trans). $\lambda_{max}(CH_2Cl_2)$/nm: 241 (log ϵ/dm^3 mol^{-1} cm^{-1} 4.72), 341 (4.91), and 421 (5.13). δ_H(400 MHz; $CDCl_3$): 1.38 (54 H, s, *t*-Bu), 7.05 and 7.19 (6 H, d, J = 16.5, cv vinyl H), 7.09 and 7.13 (6 H, ABq, J = 16, cv H), 7.14 and 7.45 (12 H, AA′BB′, cp H), 7.37 (3 H, dd, J = 1.5, sp H), 7.39 (6 H, d, J = 1.5, sp H), and 7.51 and 7.54 (12 H, AA′BB′, cp H. *m*/*z* (FAB): 1194.8 (M^+, 100%). GPC: $\bar{M}_w = 2.1 \times 10^3$ and $\bar{M}_n = 2.0 \times 10^3$.

[G-1]$_3$N, 17. A mixture of [G-1]CH_2P **6** (1.19 g, 1.89 mmol), **15** (302 mg, 0.475 mmol) and potassium *tert*-butoxide (212 mg, 1.89 mmol) in tetrahydrofuran (60 mL) was stirred at room temperature under argon for 14 h. The solvent was removed and water (25 mL) and dichloromethane (50 mL) were added. The organic layer was separated, washed with brine (100 mL), dried over anhydrous sodium sulfate, and filtered and the solvent removed to give a yellow solid. The residue was purified by column chromatography over silica using a dichloromethane−light petroleum mixture (1:4 to 1:2) to give **17** (817 mg, 81%) as a bright yellow solid, mp 238−239 °C. Anal. Calcd for $C_{162}H_{183}N$: C, 90.7; H, 8.6; N, 0.65. Found: C, 90.5; H, 8.8; N, 0.6. ν_{max}(KBr disk)/cm^{-1}: 956 (C═C−H trans). $\lambda_{max}(CH_2Cl_2)$/nm: 239 (log ϵ/dm^3 mol^{-1} cm^{-1} 4.99), 323 (5.31), 334 sh (5.29), and 423 (5.17). δ_H(400 MHz; $CDCl_3$): 1.40 (108 H, s, *t*-Bu), 7.07 and 7.15 (6 H, d, J = 16, cv H), 7.16 and 7.47 (12 H, AA′BB′, cp H), 71.8 and 7.29 (12 H, d J = 16, G-1 vinyl H), 7.20 and 7.26 (6 H, d, J = 16, cv H), 7.40 (6 H, dd, J = 1.5, sp H), 7.44 (12 H, d, J = 1.5, sp H), 7.55 and 7.58 (12 H, AA′BB′, cp H), 7.61 (6 H, br s, G-1 bp H), and 7.64 (3 H, br s, G-1 bp H). *m*/*z* (MALDI): 2143.7 (M^+, 100%). GPC: $\bar{M}_w = 3.9 \times 10^3$ and $\bar{M}_n = 3.6 \times 10^3$.

[G-2]$_3$N, 18. A mixture of [G-2]CH_2P, **10** (1.01 g, 0.80 mmol), **15** (129 mg, 0.203 mmol), and potassium *tert*-butoxide (93 mg, 0.83 mmol) in tetrahydrofuran (40 mL) was stirred at room temperature under argon for approximately 14 h. The solvent was removed by rotary evaporation. Water (25 mL) and dichloromethane (50 mL) were added. The organic layer was separated, washed with brine (100 mL), dried over anhydrous sodium sulfate, and filtered and the solvent removed to give a yellow solid. The residue was purified by column chromatography over silica using a dichloromethane−light petroleum mixture (1:4 to 1:2) to give **18** (611 mg, 76%) as a bright yellow solid, mp 268 °C. Anal. Calcd for $C_{306}H_{351}N$: C, 90.9; H, 8.75; N, 0.35. Found: C, 90.6; H, 9.2; N, 0.35. ν_{max}(KBr disk)/cm^{-1}: 957 (C═C−H trans). $\lambda_{max}(CH_2Cl_2)$/nm: 323 (log ϵ/dm^3 mol^{-1} cm^{-1} 5.73), 334 sh (5.70), and 423 (5.18). δ_H(400 MHz; $CDCl_3$): 1.41 (216 H, s, *t*-Bu), 7.08 and 7.13−7.19 (6 H, d, J = 16, cv H), 7.17 and 7.49 (12 H, AA′BB′, cp H), 7.20 and 7.32 (24 H, d, J = 16, G-2 vinyl H), 7.20−7.31 (6 H, d, J = 16, cv H, 7.33 (12 H, s, G-1 vinyl H), 7.41 (12 H, dd, J = 1.5, sp H), 7.45 (24 H, d, J = 1.5, sp H), 7.57 and 7.60 (12 H, AA′BB′, cp H), 7.67 (24 H, G-1 bp H and G-2 bp H), and 7.71 (3 H, br s, G-1 bp H). *m*/*z* (MALDI): 4042.8 (M^+, 100%). GPC: $\bar{M}_w = 6.4 \times 10^3$ and $\bar{M}_n = 5.7 \times 10^3$.

[G-3]$_3$N, 19. Potassium *tert*-butoxide (122 mg, 1.09 mmol) was added to a solution of [G-3]CH_2P, **14** (551 mg, 0.218 mmol), and **15** (34.6 mg, 0.054 mmol) in dry tetrahydrofuran (15 mL) and heated at reflux for approximately 21.5 h under argon and then the solvent was removed. Dichloromethane (50 mL) was added and the organic layer was washed with water (50 mL) and brine (50 mL), dried over anhydrous sodium sulfate, filtered, and the solvent removed to leave a yellow solid. The residue was difficult to purify by column chromatography over silica. When a dichloromethane−light petroleum mixture (1.5:3.5 to 2:3) was used a small amount of pure material could be isolated (∼90 mg). The remaining impure material (∼260 mg) and iodine (17 mg, 0.07 mmol) were dissolved in toluene (6 mL) and heated at reflux for 5.2 h. The solvent was removed and the residue purified by column chromatography over silica using a dichloromethane−light petroleum mixture (1.5:3.5 to 2:3). The main fraction was collected and the solvent removed. The residue was combined with the first fraction of pure material to give **21** (268 mg, 63%), mp 266−267 °C. Anal. Calcd for $C_{594}H_{687}N$: C, 91.0, H, 8.8; N, 0.2. Found: 90.6; H, 9.3; N, nil. ν_{max}(KBr disk)/cm^{-1}: 958 (C═C−H trans). $\lambda_{max}(CH_2Cl_2)$/nm: 239 (log ϵ/dm^3 mol^{-1} cm^{-1} 5.52), 323 (6.08), 334 sh (6.04), and 424 (5.16). δ_H(400 MHz; $CDCl_3$): 1.40 (432 H, s, *t*-Bu), 7.03−7.37 (96 H, cv H, G-1 vinyl H, G-2 vinyl H and G-3 vinyl H), 7.17 and 7.50 (12 H, AA′BB′, cp H), 7.39 (24 H, dd, J = 1.5, sp H), 7.45 (48 H, d, J = 1.5, sp H), 7.59 and 7.63 (12 H, AA′BB′, cp H), 7.65−7.77 (63 H, bp H). *m*/*z* (MALDI): 7839.4 (M^+, 100%). GPC: $\bar{M}_w = 1.0 \times 10^4$ and $\bar{M}_n = 8.8 \times 10^3$.

Acknowledgment. We thank EPSRC, Raychem and Opsys Ltd. for financial support. I.D.W.S. is a Royal Society University Research Fellow.

References and Notes

(1) Wang, P. W.; Liu, Y. J.; Devadoss, C.; Bharathi, P.; Moore, J. S. *Adv. Mater.*, **1996**, *8*, 237.

(2) Halim, M.; Pillow, J. N. G.; Samuel, I. D. W.; Burn, P. L. *Adv. Mater.* **1999**, *11*, 371.

(3) (a) Lupton, J. M.; Samuel, I. D. W.; Frampton, M. J.; Beavington, R.; Burn, P. L. *Adv. Funct. Mater.* **2001**, *11*, 287. (b) Lo, S.-C.; Male, N. A. H.; Markham, J. P. J.; Magennis, S. W.; Burn, P. L.; Salata, O. V.; Samuel, I. D. W. *Adv. Mater.* **2002**, *13*, 975. (c) Markham, J. P. J.; Lo, S.-C.; Magennis, S. W.; Burn, P. L.; Samuel, I. D. W. *Appl. Phys. Lett.* **2002**, *80*, 2645.

(4) (a) Freeman, A. W.; Koene, S. C.; Malenfant, P. R. L.; Thompson, M. E.; Fréchet, J. M. J. *J. Am. Chem. Soc.* **2000**, *122*, 12385. (b) Adronov, A.; Fréchet, J. M. J. *Chem. Commun.* **2000**, 1701. (c) Kwok, C. C.; Wong., M. S. *Macromolecules* **2001**, *34*, 6821.

(5) Lupton, J. M.; Samuel, I. D. W.; Beavington, R.; Frampton, M. J.; Burn, P. L.; Bässler, H. *Phys. Rev. B* **2001**,*63*, 5206.

(6) (a) Samuel, I. D. W.; Rumbles, G.; Friend, R. H. In *Primary Photoexcitations in Conjugated Polymers: Molecular Exciton versus Semiconductor Band Model*; Sariciftci, N. S., Ed.; World Scientific: Singapore, 1997. (b) Samuel, I. D. W.; Rumbles, G.; Collison, C. J. *Phys. Rev. B* **1995**, *52*, 11573.

(7) Jakubiak, R.; Bao, Z.; Rothberg, L. *Synth. Met.* **2000**, *114*, 61.
(8) Yan, M.; Rothberg, L. J.; Kwock, E. W.; Miller, T. M. *Phys. Rev. Lett.* **1995**, *75*, 1992.
(9) Jenekhe, A.; Osaheni, J. A. *Science* **1994**, *265*, 765.
(10) Conwell, E. M. *Phys. Rev. B* **1998**, *57*, 14200.
(11) (a) Lupton, J. M.; Samuel, I. D. W.; Burn, P. L.; Mukamel, S. *J. Phys. Chem. B* **2002**, *106*, 7647. (b) Lupton, J. M.; Samuel, I. D. W.; Burns, P. L.; Mukamel, S. *J. Chem. Phys.* **2002**, *116*, 455.
(12) (a) Meier, H.; Lehmann, M. Kolb, U. *Chem.—Eur. J.* **2000**, *6*, 2462. (b) Deb, S. K.; Maddux, T. M.; Yu, L. *J. Am. Chem. Soc.* **1997**, *119*, 9079. (c) Segura, J. L.; Gómez, R.; Martín, N.; Guldi, D. M. *Org. Lett.* **2001**, *3*, 2645.
(13) Pillow, J. N. G.; Halim, M.; Lupton, J. M.; Burn, P. L.; Samuel, I. D. W. *Macromolecules* **1999**, *32*, 5985.
(14) Bollinger, M. J. M.; Comisarow, M. B.; Cupas, C. A.; Olah, G. A. *J. Am. Chem. Soc.* **1967**, *89*, 5687.
(15) Wieland, H. *Chem. Ber.* **1907**, 4278.
(16) Burn, P. L.; Beavington, R.; Frampton, M. J.; Pillow, J. N. G.; Halim, M.; Lupton, J. M.; Samuel, I. D. W *Mater. Sci. Eng. B* **2001**, *85*, 190.
(17) Varnavski, O.; Leanov, A.; Liu, L.; Takacs, J.; Goodson, T., III. *Phys. Rev. B* **2000**, *61*, 12732.
(18) (a) Varnavski, O.; Menkir, G.; Samuel, I. D. W.; Lupton, J. M.; Beavington, R.; Burn, P. L.; Goodson, T., III. *Appl. Phys. Lett.* **2000**, *77*, 1120. (b) Varnavski, O.; Samuel, I. D. W.; Pålsson, L.-O.; Beavington, R.; Burn, P. L.; Goodson, T., III. *J. Chem. Phys.* **2002**,*116*, 8893.
(19) (a) Poliakov, E. Y.; Chernyak, V.; Tretiak, S.; Mukamel, S. *J. Chem. Phys.* **1999**, *110*, 8161. (b) Tretiak, S.; Chernyak, V.; Mukamel, S. *J. Phys. Chem. B* **1998**, *102*, 3310.
(20) Swallen, S. F.; Kopelmann, R.; Moore, J. S.; Devadoss, C. *J. Mol. Struct.* **1999**, *485−486*, 585.
(21) Lupton, J. M.; Samuel, I. D. W.; Beavington, R.; Burn, P. L.; Bässler, H. *Synth. Met.* **2001**, *116*, 357.
(22) Lupton, J. M.; Samuel, I. D. W.; Beavington, R.; Burn, P. L.; Bässler, H. *Adv. Mater.* **2001**, *13*, 258.
(23) Jansen, J. F. G.; DeBrabandder-Vandenberg, E. M. M.; Meijer, E. W. *Science* **1994**, *266*, 1226.
(24) Pope, M.; Swenberg, C. E *Electronic Processes in Organic Crystals and Polymers*, 2nd ed.; Oxford University Press: Oxford, U.K., 1999.
(25) Perrin, D. D.; Amarego, W. L. F. *Purification of Laboratory Compounds*; Pergamon Press: Oxford, U.K., 1988.
(26) Gritzner, G.; Kuta, J. *Electrochim. Acta* **1984**, *29*, 869.
(27) Williams, A. T. R.; Winfield, S. A.; Miller, J. N. *Analyst* **1983**, *108*, 1067.
(28) Greenham, N. C.; Samuel, I. D. W.; Hayes, G. R.; Phillips, R. T.; Kessener, Y. A. R. R.; Moratti, S. C.; Holmes, A. B.; Friend, R. H. *Chem. Phys. Lett.* **1995**, *241*, 89.

MA011996G